

MODELLING INUNDATION EXTENTS OF THE JUNE 2016 STORM SURGE IN ESTUARINE ENVIRONMENTS USING STATIC AND DYNAMIC APPROACHES

K Kumbier^{1,2}, R C Carvalho², A T Vafeidis¹, C D Woodroffe²

¹University of Kiel, Kiel, Germany

²University of Wollongong, Wollongong, NSW

Abstract

Identification of areas exposed to storm-tide inundation is of importance for coastal flood risk management. In June 2016 the coincidence of a storm surge with a high spring tide caused severe inundation across the coast of NSW. Settlements in low-lying areas of estuarine environments were particularly at risk due to the potential enhancement of extreme water levels by riverine flooding. Traditional flood risk assessments do not account for the latter driver, even though the degree of impact on flood extent can vary with the catchment size of an estuarine environment.

This study compares flood extent generated from static (“bathtub”) and dynamic (Delft3D) modelling approaches in two wave-dominated barrier estuaries (Shoalhaven Estuary and Lake Illawarra) at different stages of infill, tidal modification and catchment size. Observed water levels of the June 2016 storm surge were used to force the models, whereas observational data such as satellite imagery, aerial photography, tidal gauges and water level logger measurements were used to validate modelling results. Modelling differences in flood extent between the two approaches were smallest in Lake Illawarra (0.2 km²), where riverine discharge appeared to be negligible. At the Shoalhaven estuary modelling differences were larger (11 km²) and the consideration of river discharge through dynamic modelling techniques was shown to be crucial for the modelling of observed water levels and flood extents, because storm-tide inundation and riverine flooding appeared to coincide. In conclusion, results show that the static “bathtub” modelling is an efficient management approach to map flood extent at low cost and low computational expenses in wave-dominated barrier estuaries at youthful/intermediate stages of infill and similar catchment area (<1000 km²) to Lake Illawarra, such as Lake Macquarie or St. Georges Basin.

Introduction

Storm surges are the main driver of coastal flooding leading to loss of human life, destruction of homes and civil infrastructure (Resio and Westerink, 2008). An increase in sea level is expected to exacerbate storm surge related risks to coastal communities, because the frequency and extent of coastal flooding is likely to increase (IPCC, 2014; Vitousek et al., 2017). Furthermore, the impacts of a storm surge may intensify when it coincides with high spring tide (Pugh, 2004) and/or riverine flooding (Zheng et al., 2013). Extreme water levels resulting from a combination of storm-tide flooding and riverine flooding are also known as coincident or compound flood events (IPCC, 2014; Leonard et al., 2014). For some time the two types of flooding have been treated independently in coastal flood risk assessments (Torres et al. 2015), even though joint-probability analysis highlighted significant dependence between extreme rainfall and extreme storm surges along the east coast of Australia (Zheng et al., 2013).

A key component of any flood risk assessment is the preparation of flood maps, which aim to identify coastal areas threatened by flooding. These maps can be generated through static and dynamic modelling approaches. The static modelling approach, also referred to as “bathtub”, “planar” or “bucket-fill” method, has been used widely because of its ability to simply and quickly generate maps of flood extent using a Geographical Information System (GIS) at comparatively low computational costs and time (Poulter and Halpin, 2008; Van de Sande et al., 2012; Seenath et al., 2016). The approach is based on the assumption that areas lower than a certain water level are inundated if there is hydrological connectivity. Static flood models allow only for a specific extreme water level as an input and not spatially varying water levels from different flooding drivers such as those resulting from storm surge and riverine discharges. The static model generally overestimates flood extents due to the omission of important factors influencing floodwater flow such as bottom friction, the conservation of mass and flood duration (Bates et al., 2005; Breilh et al., 2013; Seenath et al., 2016; Ramirez et al., 2016; Vousdouskas et al., 2016).

The dynamic modelling approach utilizes a hydrodynamic model to simulate the flow of floodwater resulting from various sources such as storm surges and/or riverine discharges. A drawback of the dynamic modelling is the more complex model setup and significantly longer computational times, which vary with the level of complexity of the applied model. A comprehensive overview of different flood inundation modelling approaches, as well as recent developments can be found in Teng et al. (2017). Dynamic flood models such as Delft3D, Lisflood-FP or Telemac have been applied in several studies where they consistently demonstrated a satisfactory predictive skill (Bates et al., 2005, Ramirez et al., 2016, Seenath et al., 2016, Vousdouskas et al., 2016). Comparative studies of static and dynamic modelling approaches suggest on one hand to avoid the use of static models in areas of flat topography, and on the other hand, to apply them in narrow low lands in estuaries or back barrier lagoons (Breilh et al., 2013; Ramirez et al., 2016). However, to our knowledge no study has related modelling differences to estuarine classification schemes, even though process based classification schemes may indicate how the floodplains of an estuarine system are shaped and which flooding types are affecting it.

Roy et al. (2001) classified the fundamentally different types of estuaries in NSW based on two criteria: First, in accordance with their inheritance of different coastal settings that create distinct estuary types and second, differing rates of sediment infilling that determine how far along their evolutionary continuum the present-day estuaries have progressed. In the context of flood modelling and coastal flood risk assessment, classification schemes such as those of Roy et al. (2001) may help to decide which flood modelling approach to use in certain estuarine environments.

In this paper we present a comparison of static (GIS) and dynamic (Delft3D) modelled flood extents for two estuaries, in order to guide coastal flood risk assessment in estuarine environments. Therefore, the mapping of flood extent due to the June 2016 East Coast Low (ECL) is compared in two wave-dominated barrier estuaries at a different stage of infill, tidal modification and catchment size.

Study sites

The two study sites chosen for this comparative analysis are located in southeast Australia. Hydrodynamically the coast is controlled mainly by waves. Tides are semi-diurnal with a maximum spring tidal range of 2 m at the open coast (Roy et al., 2001). The tidal signal displays a significant diurnal inequality and spatially varies with a decrease of 0.2 m towards southern NSW (Morris et al., 2013). In terms of their infilling

stage, floodplain shape and hydrodynamics, Lake Illawarra and the Shoalhaven Estuary are comparatively contrasting estuarine systems.

Lake Illawarra (Fig. 1) has been categorized as a wave-dominated barrier estuary of intermediate evolutionary stage (Roy et al., 2001). The shallow tidal lake of 36 km² water area has an average depth of 1.7 m and a maximum depth of about 4 m. The system receives runoff from two principal catchments totalling an area of approximately 235km². The infilling of the estuary is driven by marine and fluvial processes, which create distinct facies with fluvially-influenced deltas propagating into the estuary at Macquarie Rivulet and Mullet Creek, and a marine-influenced flood-tide delta propagating into the estuary through the entrance channel (Sloss et al., 2004; Short and Woodroffe, 2009). The lowest elevated areas of the floodplain are located surrounding the deltas of Macquarie Rivulet and Mullet Creek. The entrance of Lake Illawarra was intermittently closed and open to the ocean, but training works in 2007 stabilised and permanently opened the entrance (Wiecek et al., 2016). Nowadays tides in the estuary are strongly attenuated once the tidal wave travels through the narrow constrained entrance channel. The entrance gauge displays an average spring tidal range of approximately 1 m, but decreases to 0.2 m at Cudgeree Bay, which is 2.5 km from the Entrance gauge (MHL, 2012). After this attenuation, the spring tidal range remains quite stable between 0.15 m and 0.2 m through the estuary.

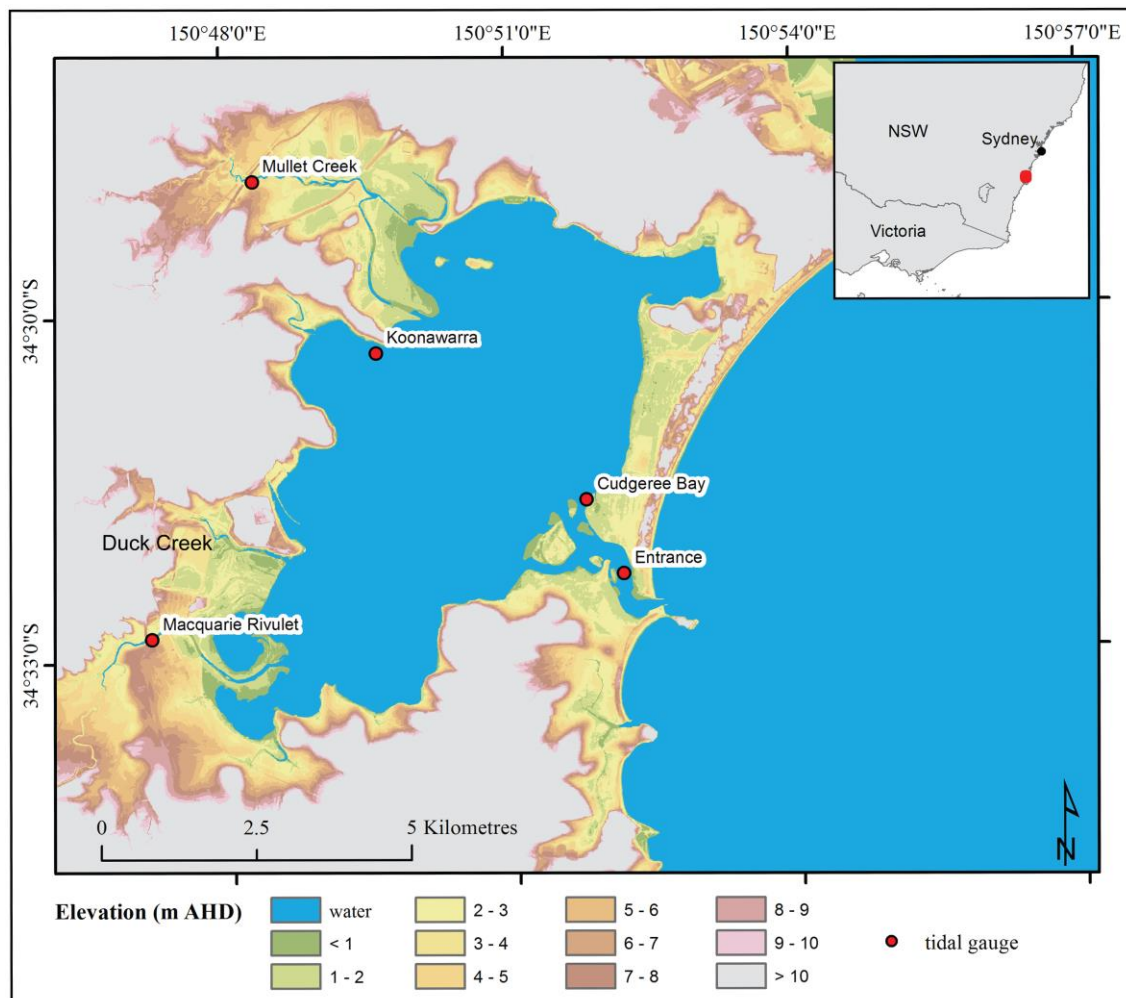


Figure 1: Map showing Lake Illawarra and tidal gauges (red dots) in the study area. LiDAR derived topographic data of the floodplain is presented in m AHD.

The Shoalhaven Estuary occurs in the lower reaches of the Shoalhaven River, which is one of the largest rivers on the south coast of NSW. The estuary has been categorized as a wave-dominated barrier estuary of mature evolutionary stage (Roy et al., 2001). The estuarine infilling during the past 6000 years gave the estuary today's shape and its characteristic low-lying alluvial plains (Woodroffe et al., 2000). The Shoalhaven River drains a catchment area of 7150 km² and is regulated by Tallowa dam, which is located approximately 68 km upstream from the coast. Broughton Creek is the largest tributary in the northern part of the floodplain, while the southern part is drained by the much smaller Crookhaven River (Fig. 2). The waterway of the Shoalhaven Estuary is quite unusual with a permanent opening at Crookhaven Heads and an intermittent entrance at Shoalhaven Heads. This environmental setting of two entrances of different nature results from the construction of Berrys Canal by landowner Alexander Berry in 1822. Originally the estuary had its opening to the Pacific Ocean at Shoalhaven Heads, but with the construction of Berrys Canal the discharge has been redirected towards Crookhaven Heads, which is more protected from wave action and permanently open. In consequence, Shoalhaven Heads turned into an intermittent opening, which only breaches during large storm events (Carvalho and Woodroffe, 2014). The average spring tidal range at Greenwell Point is approximately 1.4 m and just slightly attenuated towards Shoalhaven Heads and Nowra (0.2 m). Further upstream the tide displays even a small amplification (MHL, 2012).

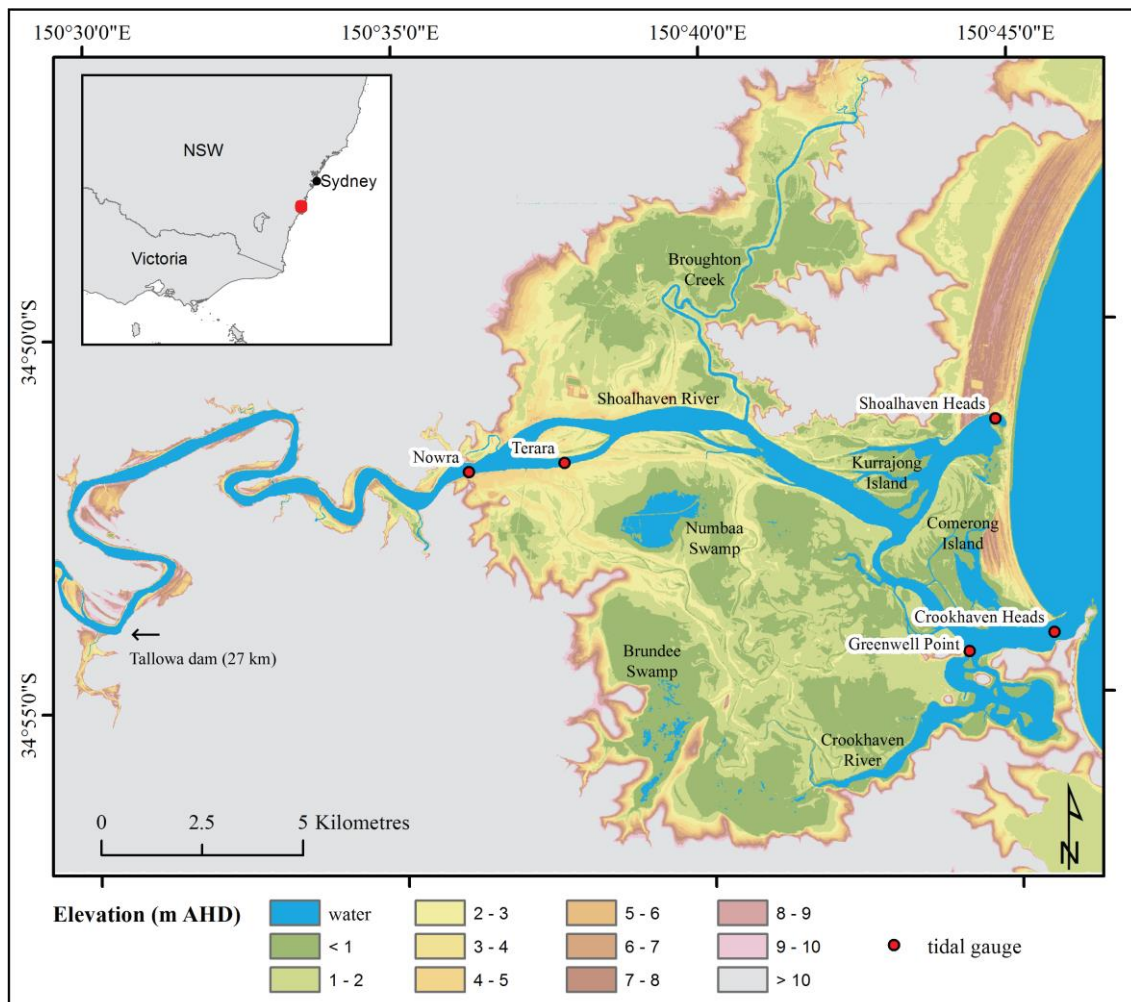


Figure 2: Map showing the Shoalhaven Estuary and tidal gauges (red dots) in the study area. LiDAR derived topographic data of the floodplain is presented in m AHD.

In June 2016 a storm event caused a positive storm surge and severe inundation of the floodplains surrounding Lake Illawarra and the Shoalhaven Estuary. The storm was due to an East Coast Low (ECL), which formed northeast of Queensland and tracked south along the eastern coastline of Australia. It was characterised by strong winds and heavy rainfall up to 289 mm (weekly cumulative value) at nearby Wollongong (Burston et al., 2016).

Data and methods

Data sets representing water levels, elevation, bathymetry, land use, river discharge and wind were used to assess the extent of flooding at the study sites. Aerial photographs, two satellite images and two water-level loggers were used to validate modelled flood extents and evaluate model performance.

The Light Detection and Ranging (LiDAR) elevation data set were provided as digital elevation models (DEM) and downloaded from the server of Geoscience Australia (<http://www.ga.gov.au/elvis/>). These DEMs have a spatial resolution of 5 m, are vertically referenced to Australian Height Datum (AHD) and reported to have a vertical accuracy of at least 0.3 m (95% confidence) and a horizontal accuracy of at least 0.8 m (95% confidence). Bathymetric data consisting of point measurements taken during hydrographic surveys between September 2005 and November 2006 for the Shoalhaven Estuary and August to September 2007 for Lake Illawarra were provided and downloaded from the Office of Environment and Heritage (OEH) (<http://www.environment.nsw.gov.au/estuaries/list.htm>). These point measurements were interpolated to raster surfaces of 5 m spatial resolution using an ordinary Kriging method with a spherical semivariogram model. The accuracy of this interpolation was verified by comparison of random subsets of point measurements to interpolated cell values.

Water level measurements at 15 min intervals for 4 tidal gauges in Lake Illawarra and 5 tidal gauges in the Shoalhaven Estuary were provided by the OEH through Manly Hydraulics Laboratory. River discharge measurements at 15 min intervals for the Shoalhaven River and Macquarie Rivulet were provided by NSW Water. Measurements of average wind speed and direction for nearby Port Kembla station were provided and downloaded from the Bureau of Meteorology (<http://www.bom.gov.au/oceanography/projects/absImp/data/>).

The land use data were obtained from the NSW Department of Environment and Climate Change (<http://data.environment.nsw.gov.au/dataset/nsw-landuseac11c>). They were used to create a file of spatially varying bottom friction. Therefore, friction coefficients were taken from literature (Chow, 1959; Fisher and Dawson, 2011; Kaiser et al., 2011) and assigned to the land use data using a GIS.

The areas flooded during the June 2016 ECL were determined by using Sentinel-1 Synthetic Aperture Radar (SAR) imagery (Copernicus Sentinel Data, 2016), which was downloaded using the USGS Earth Explorer (<https://earthexplorer.usgs.gov/>). The imagery was taken on 6 June 2016 at 19:15. Inundated areas were identified through processing of the VH polarization band using the open source software SNAP toolbox (<http://step.esa.int/main/download/>). The SAR imagery was radiometrically calibrated, terrain corrected, speckle filtered and reclassified based on the distribution of backscattering signals. It was possible to separate the imagery into dry and inundated pixels based on the different reflection of wet and dry areas. The resulting raster data set of the observed flood extent in the Shoalhaven Estuary was visually compared and adjusted using 75 oblique aerial photographs of the flood extent. Examples of photographs of the flood extent observed in the Shoalhaven Estuary are shown in Fig. 3.

The photographs were taken during a helicopter survey on 6 June around 17:00 by the Shoalhaven City Council. In addition, a Landsat 8 image provided by the U.S. Geological Survey (downloaded using the USGS Earth Explorer), taken on 6 June at 23:45, was used to further identify inundated areas and visually verify the SAR imagery reclassification.

Measurements from two water-level loggers (HOBO® U20-001-04) at Comerong Island in the Shoalhaven Estuary were used to validate wetting and drying processes of the dynamic model.

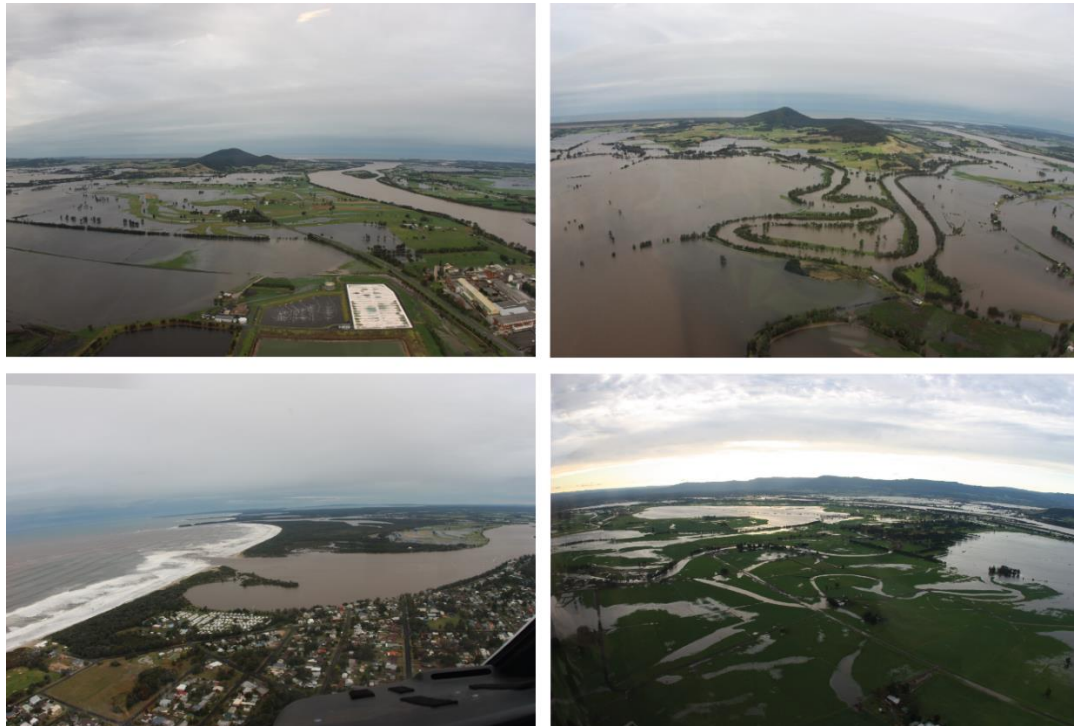


Figure 3: Selection of aerial photographs taken by the Shoalhaven City Council on 6th of June 2016 around 17:00h showing flood extent of the June 2016 storm event in the Shoalhaven Estuary.

Static modelling approach

The static flood model uses a Geographic Information System (GIS) to map the extent of flooding for a particular extreme water level. The flood extents for both estuaries were calculated by geographical selection of inundated DEM locations, which were less than or equal to the observed peak water level at the entrance of the estuaries (1.496m at Lake Illawarra and 1.653m at the Shoalhaven Estuary). This selection was further limited to areas, which are in direct connection to the estuary or connected by creeks in order to ensure hydrological connectivity (as presented in Poulter and Halpin, 2008; Van de Sande et. al., 2012). Only pixels with a direct or indirect (eight neighbour cells) connection to the ocean were assumed to be inundated. Finally the maximum flood extents were calculated by the number of pixels belonging to the flood extent and the known pixel dimensions.

Dynamic modelling approach

The hydrodynamic numerical module Delft3D-Flow of the open source model Delft3D (Deltares, 2014) was used to simulate the resulting hydrodynamics using a combination of storm-tide and riverine discharge recorded for the June 2016 storm event. The finite difference model was carried out in a depth-averaged mode (2D) to solve the unsteady shallow water equations on a rectangular grid.

Figure 4 illustrates the dynamic model setup for both study sites. The computational grid for Lake Illawarra was set to a spatial resolution of 10 m while the Shoalhaven Estuary was modelled using a 25 m grid. The open boundary of the Illawarra model was forced with time-series of water level measurements taken at the entrance gauge, whereas the discharge location was forced with time-series of discharge measurements taken at Macquarie Rivulet. No discharge data was available for Mullet Creek.

The Shoalhaven model was defined with two open boundaries (Crookhaven Heads and Shoalhaven Heads, because of the breaching of the intermittent entrance in Shoalhaven Heads during the storm. These boundaries were forced with time-series of water level measurements taken at Crookhaven Heads gauge. The discharge measurements of the Shoalhaven River were used to force the upstream boundary of the model. The performance of both models was assessed by comparison of modelled and observed water levels at 4 monitoring points (Fig.4 – red dots). Water-level loggers were located at Comerong Island in the Shoalhaven estuary (Fig.4 – orange dots). The maximum observed flood extent is indicated in dark blue (Fig. 4).

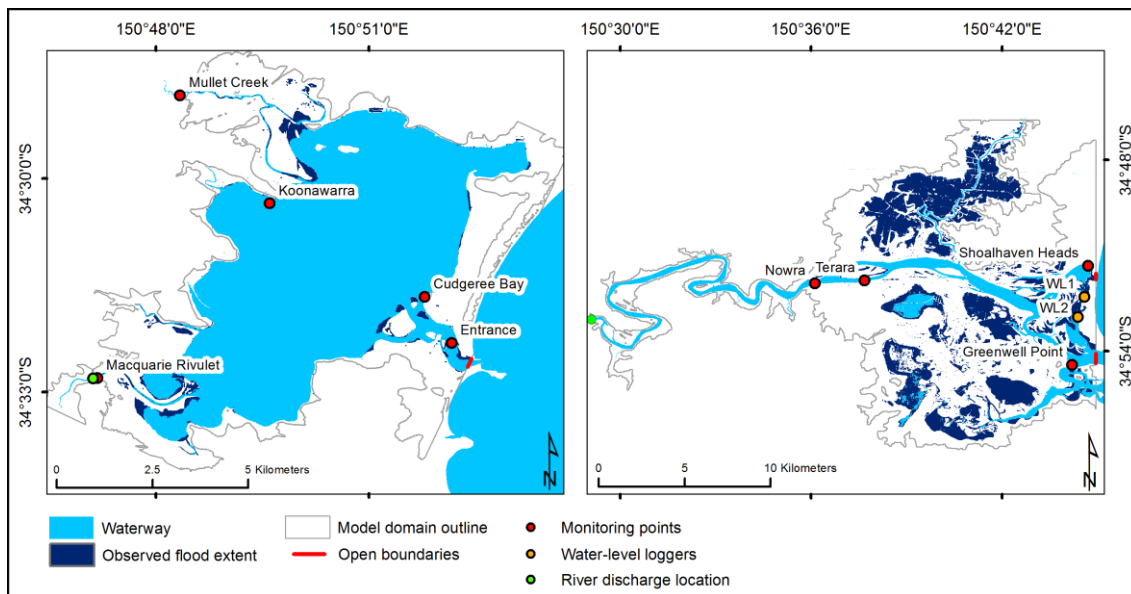


Figure 4: Map showing the hydrodynamic model domains (grey outline), open boundaries (bold red lines), the river discharge locations (green dots) and monitoring points corresponding to tidal gauges (red dots) as well as water-level loggers (orange dots). The observed flood extent of the June 2016 ECL is indicated in dark blue.

Simulations of flooding due to the June 2016 ECL were carried out including and excluding river discharges in order to assess their impact on modelled flood extents. All simulations were executed on a computer with an Intel Xeon E5-2670 processor with 12 cores and resulted in computations times of 42 h for the Shoalhaven model and 19 days for the Illawarra model.

Percentages of the model's correct estimations, overestimations and underestimations were derived through normalization of the three categories by the observed flood extent (as presented in Ramirez et al., 2016).

Results and Discussion

Dynamic modelling

Comparison of observed (blue) and modelled water levels (red and black) of the dynamic model for Lake Illawarra and the Shoalhaven Estuary are presented in Figure 5 and 6. Red lines correspond to the simulation including riverine discharge of Macquarie Rivulet, whereas black lines correspond to the simulation without riverine discharge.

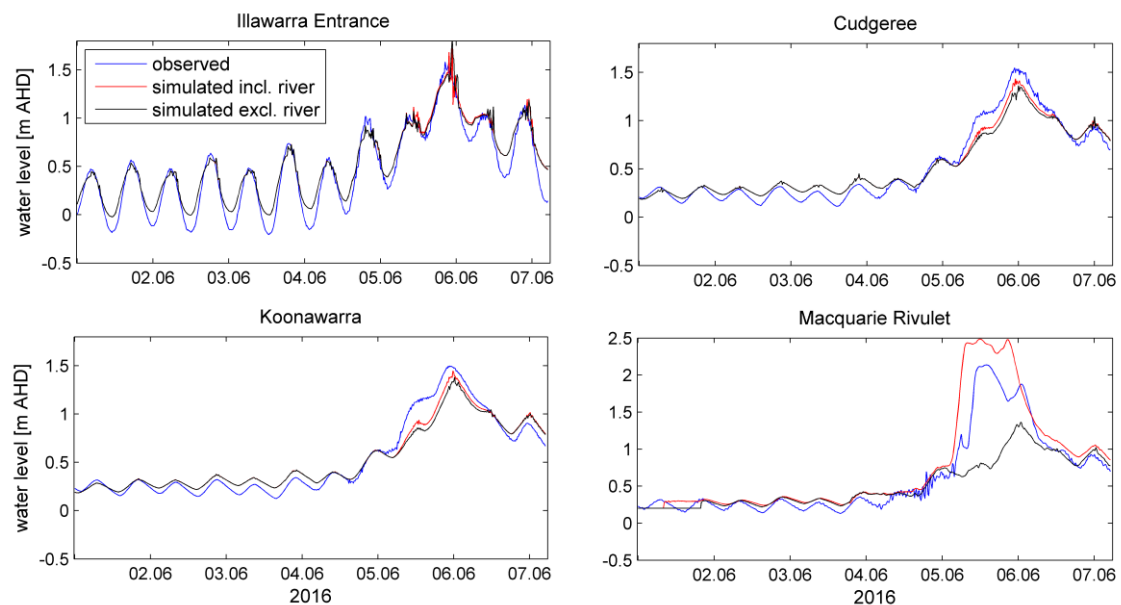


Figure 5: Observed (blue) and modelled water levels (red and black) for monitoring points in Lake Illawarra. Observed water levels from OEH.

The modelling of water levels at the entrance of Lake Illawarra showed small instabilities and an underestimation of the tidal range. These instabilities likely result from a too large computational time step and the location of the open boundary, whereas the underestimation of the tidal range may result on one hand from the chosen location of the open boundary, and on the other hand, from changes in the bathymetry of the entrance channel. The entrance channel of Lake Illawarra has reportedly changed between the hydro survey in 2008 and the ECL in 2016 (Regana, 2016; Wiecek et al., 2016), as the channel continues to scour in adjusting to the continuously open entrance (Couriel et al., 2013). Peak water levels in Cudgeree Bay and Koonawarra were underestimated by approximately 0.05 m. This may on one hand relate to the underestimation in tidal range at the entrance and on the other hand to the non-consideration of the discharge of Mullet Creek. The modelled water level prediction for Macquarie Rivulet differed from observed ones, because the creek bathymetry was represented by inaccurate topographic data. Nevertheless, high correlations between modelled and observed water levels at all monitoring points in Lake Illawarra indicate that the ECL event was replicated reasonably well by the dynamic model. Statistical measures of r^2 and RMSE of 0.97 and 0.12 m for Illawarra Entrance, 0.98 and 0.08 m for Cudgeree Bay, 0.98 and 0.09 m for Koonawarra and 0.95 and 0.26 m for Macquarie Rivulet confirm this. The inclusion of riverine discharge showed to be of importance for

the replication of the water level at Macquarie Rivulet, but the additional water volume had only a low impact on water levels measured in Koonawarra and Cudgeree Bay. Consideration of riverine discharge elevated the water level in Koonawarra and Cudgeree Bay by only 6 cm. The increase in flood extent of 0.1 km² (2.5 %) was also fairly small (Table 1). Unfortunately, no discharge data was available for Mullet Creek. Follow up research should incorporate this data in order to explore its influence on lake water levels and flood extent. Considering the catchment size of Mullet Creek, an inclusion of this discharge is likely to add another 5-6 cm to the lake water level.

Table 1: Dynamically modelled flood extent (in km²) including and excluding riverine discharge.

	dynamic model	
	incl. river	excl. river
Lake Illawarra	4.0	3.9
Shoalhaven Estuary	68.6	47.9

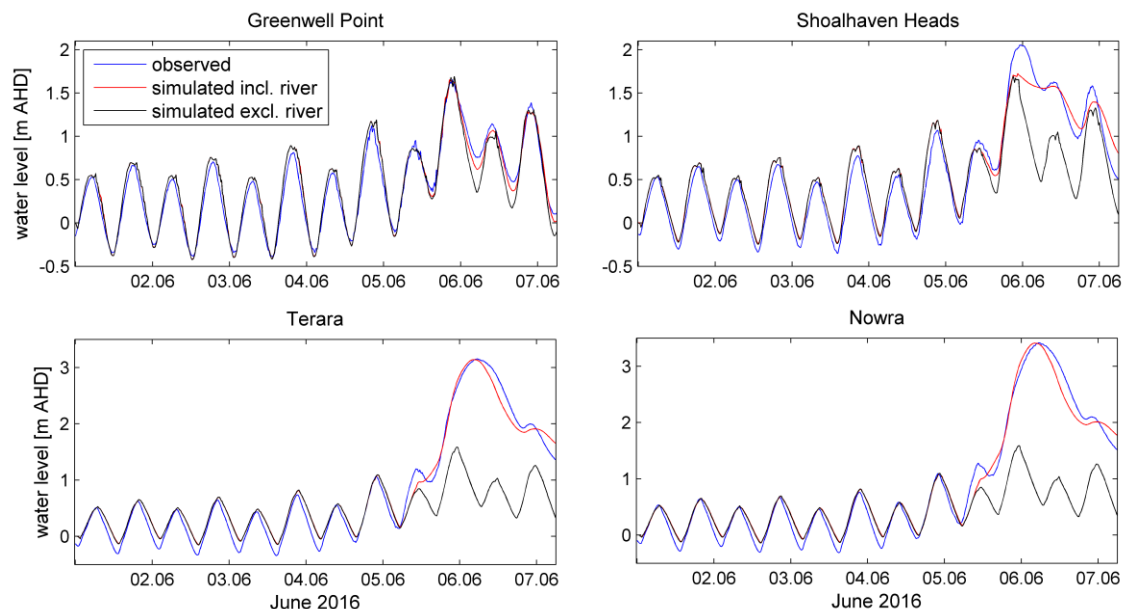


Figure 6: Observed (blue) and modelled water levels (red and black) for monitoring points in the Shoalhaven Estuary. Observed water levels from OEH.

The modelling of water levels at the Shoalhaven Estuary revealed some insights into how riverine discharge and storm-tide interacted during the June 2016 ECL. High correlations between observed and modelled water levels including riverine discharge indicate that the present dynamic model is able to replicate the involved processes. Statistical measures of r^2 and RMSE of 0.98 and 0.09 m for Greenwell Point, 0.98 and 0.14 m for Shoalhaven Heads, 0.99 and 0.15 m for Terara and 0.99 and 0.15 m for Nowra confirm this. The difference between modelled and observed peak water level was none for Greenwell Point and Nowra, -0.33 m for Shoalhaven Heads and 0.01 m for Terara. The exclusion of discharge led to large underestimations in modelled water levels at the upstream locations of Nowra and Terara (up to 2 m). The underestimation of peak water level by -0.33 m at Shoalhaven Heads indicates that forces different from those considered in the present model affected water levels. Miller et al. (2006) reported that wave action can raise water levels at Shoalhaven Heads leading to an enhancement of the flood tide. This is possible once the entrance is opened and consistent with findings of Nielsen and Hanslow (1995) for wave-setup at other NSW

river entrances. Similar influences of wave action on water levels at the mouth of an estuary were observed by Olbert et al. (2017) at the Lee River estuary in Ireland. A difference of 20.7 km² (30%) in flood extent between the discharge and no-discharge simulations further demonstrates the importance to consider river discharge when modelling storm-tide flood extents in the Shoalhaven Estuary (Table 1).

Comparison of static and dynamic approaches

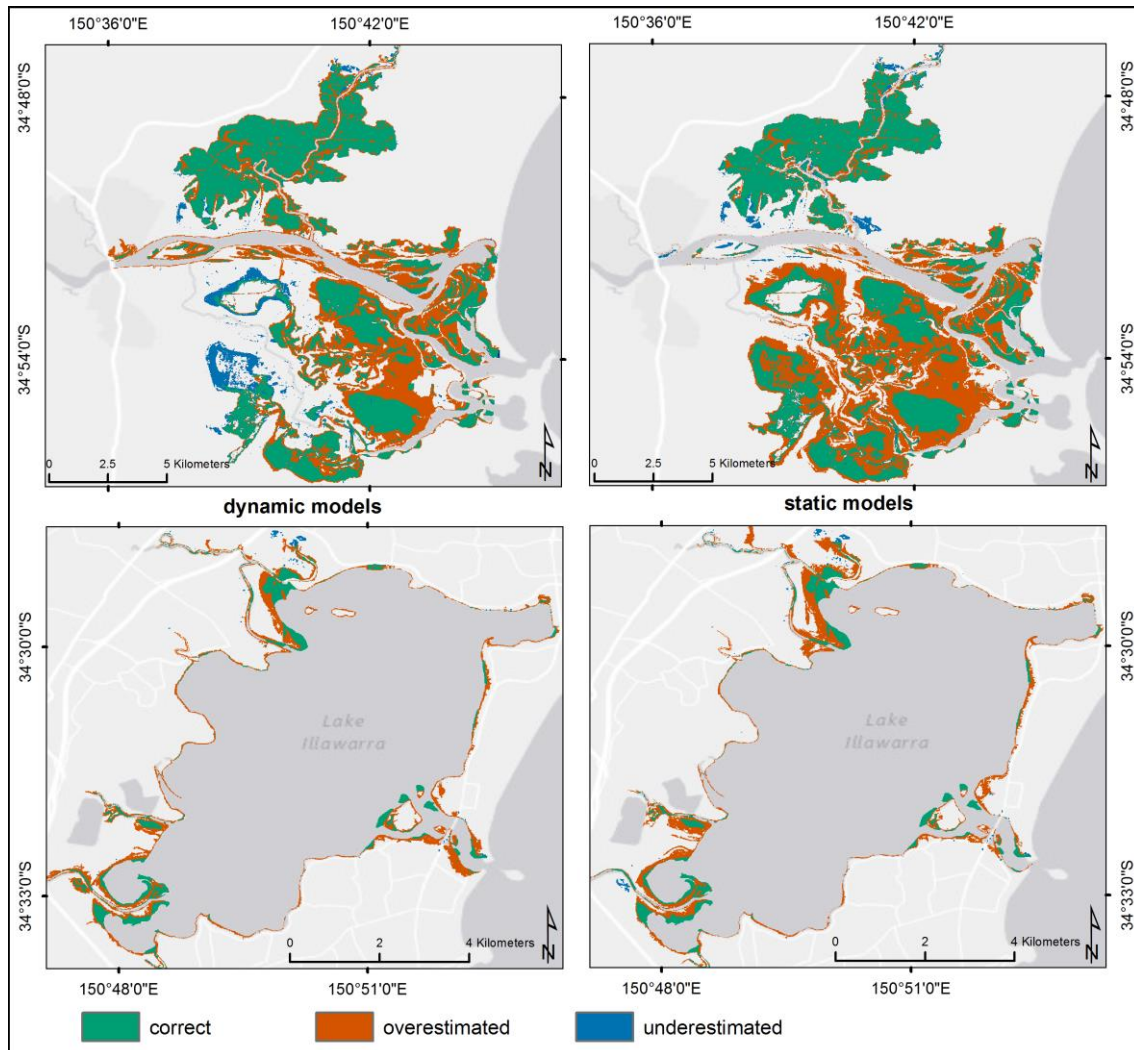


Figure 7: Locations correctly estimated (green), underestimated (blue) and overestimated (red) by static and dynamic modelling approaches in the Shoalhaven Estuary (top) and Lake Illawarra (bottom).

The June 2016 ECL inundated approximately 1.5 km² of the floodplain in Lake Illawarra (Fig. 4 and 7). The area corresponding to categories displayed in Figure 7 can be found in Table 2. Most of the flooding identified in the SAR imagery for Lake Illawarra was concentrated around the main tributaries Macquarie Rivulet, Duck Creek and Mullet Creek. The dynamic model correctly represented 94.1 % of the observed flood extent (Fig. 7, bottom left). Overestimations were equal to 175.8 % and located mainly around Macquarie Rivulet, Duck Creek and Mullet Creek. Underestimations of 5.9% in the dynamic flood extent were located mainly around Hooka Creek. The flood extent derived by the static model was 0.2 km² (5 %) larger than the dynamic modelling flood extent.

The static model correctly represented 92.4% of the observed flood extent and in turn underestimated an area equal to 7.6% (Fig. 7, bottom right). The locations correctly estimated are the same as predicted by the dynamic model. Underestimations are similar to the dynamically modelled ones, even though one patch flanking Macquarie Rivulet was not predicted as flooded. The overestimations of the static model were 187.6 %. These large overestimations result most likely from the non-identification of areas inundated less than 0.25 m and vegetation like reflectance of saltmarsh and mangrove habitats in the SAR imagery. Further the reflectance of water from sealed urban areas in the SAR imagery limited the separation of wet and dry areas.

The observed flood extent at the Shoalhaven Estuary had a size of approximately 43.5 km². The dynamic model correctly represented 89.8 % of the observed flood extent, which included most of the northern Broughton Creek floodplain and the largest patches of observed flooding in the southern Crookhaven floodplain (Fig. 7, top left). Overestimations of modelled flooding were equal to 68 %. Most of these overestimations were located in the Crookhaven floodplain surrounding Greenwell Point, as well as on Comerong and Kurrajong Islands. Underestimations of 10.2 % in modelled flood extent were located mainly in Brundee and Numbaa Swamp in the Crookhaven floodplain. The flood extent derived by the static model was 11.3 km² (16 %) larger than the dynamic modelling flood extent (Fig. 7, top right). The static model correctly represented 88.8 % of the observed flood extent, whereas underestimations were equal to 11.2 %. Overestimations of the static model were equal to 89.5 % of observed flooding and mainly located in the Crookhaven floodplain. Again, these overestimations most likely relate to the non-identification of areas inundated less than 0.25 m and vegetation-like reflectance of wetlands in the SAR imagery. When comparing these modelling approaches, one should have in mind that only the dynamic model considered the riverine discharge. Comparison of storm-tide only flood extents highlights a difference of 31 km² (40 %) between static and dynamic models.

Table 2: Observed flood extent and areas correctly estimated, overestimated and underestimated by static and dynamic models.

	Observed flood extent (km ²)	Modelled flood extent (km ²)	Correct (%)	Over (%)	Under (%)
<i>Lake Illawarra</i>					
dynamic model	1.5	4.0	94.1	175.8	5.9
static model	1.5	4.2	92.4	187.6	7.6
<i>Shoalhaven Estuary</i>					
dynamic model	43.5	68.6	89.8	68.0	10.2
static model	43.5	79.9	88.8	89.5	11.2

In summary, modelling differences in flood extent between static and dynamic approaches at Lake Illawarra were marginal (0.2 km² / 5 %). Further the inclusion of riverine discharge in the dynamic modelling was just inconsiderably affecting lake water levels (0.06 m) and flood extent (0.1 km² / 2.5%). In contrast, modelling differences at the Shoalhaven Estuary were comparatively large (11 km² / 16 %) and increased, when riverine discharge was excluded from dynamic modelling (31 km² / 40 %). This increase in modelling differences most likely relates to the disregard of bottom friction in the static approach, and demonstrates the urgent need to consider these forces in floodplains of flat topography.

Overall modelling differences between the presented approaches most likely relate to geomorphological features such as catchment characteristics and infilling stages. In this context, the catchment size of an estuary and its response time to extreme rainfall may determine if riverine discharges have to be considered when mapping flood risk. Further the infilling stage may indicate how the floodplain of an estuary is shaped. While estuaries of youthful infilling stage may be characterised by comparatively narrow floodplains, similar to those suggested for static modelling by Breihl et al. (2013) and Ramirez et al. (2016), mature systems are likely to be characterised by wide floodplains of flat topography, which require a consideration of landscape roughness through dynamic modelling. Therefore, geomorphological estuarine classifications such as Roy et al. (2001) may guide which flood modelling approach to use for the management and mapping of flood risk in estuarine environments.

Follow up research should analyse storm surges with different characteristics (e.g. magnitude and duration) than the June 2016 ECL, to further validate the presented findings. This can be challenging, because the availability of suitable data to validate hydrodynamic modelling results is known to be limited. To ensure that future storm events are recorded in a comprehensive manner, it is recommended to collect observational data of storm events in an organized way similar to Haigh et al. (2015). The aerial photographs provided by the Shoalhaven City Council were an important component of the validation data in this research.

Conclusion

The static “bathtub” modelling is an efficient management approach to map flood extent at low cost and low computational expenses in wave-dominated barrier estuaries at youthful/intermediate stages of infill and similar catchment area (<1000km²) to Lake Illawarra, such as Lake Macquarie or St. Georges Basin.

Results from the Shoalhaven Estuary demonstrate that storm-tide and riverine flooding have to be considered jointly when managing and mapping flood risk in wave-dominated barrier estuaries at mature stages of infill and similar catchment area (>6000km²) to the Shoalhaven estuary, such as the Clarence River, Manning River or Hunter River. Furthermore, the wide floodplains of flat topography require a consideration of landscape roughness.

Acknowledgement

We thank Kerrylee Rogers and Kirti Lal for the provision of water-level logger measurements. K. Kumbier expresses gratitude to the German Academic Exchange Service (DAAD) for supporting his MSc project with a scholarship.

References

Bates, PD & Dawson, RJ & Hall, JW & Horritt, MS & Nicholls, RJ & Wicks, J & Hassan, MAAM 2005, ‘Simplified two-dimensional numerical modelling of coastal flooding and example applications’, *Coastal Engineering*, vol. 52, pp. 793–810.

Breilh, JF & Chaumillon, E & Bertin, X & Gravelle, M 2013, 'Assessment of static flood modeling techniques. Application to contrasting marshes flooded during Xynthia (western France)', *Natural Hazards and Earth System Sciences*, vol. 13, pp. 1595–1612.

Burston, J & Taylor, D & Garber, S 2016, 'Contextualizing the return period of the June 2016 East Coast Low: Waves, water levels and erosion', In *25th Coastal Conference*, Coffs Harbour, accessed 12 February, <<https://www.coastalconference.com/2016/papers2016/J Joanna%20Burston%20Full%20Paper.pdf>>.

Carvalho RC & Woodroffe CD 2014, 'The sediment budget as a management tool: The Shoalhaven coastal compartment, southeastern NSW, Australia', In *23rd Coastal Conference*, Shoalhaven, accessed 15 July 2017, <<http://www.coastalconference.com/2014/papers2014/Rafael%20C.%20Carvalho%20Full%20Paper.pdf>>.

Chow, VT 1959, 'Open channel hydraulics', New York, McGraw-Hill.

Copernicus Sentinel Data 2016, '*Sentinel-1 satellite imagery retrieved from USGS Earth Explorer*', accessed 29 October 2016, <<https://earthexplorer.usgs.gov/>>.

Couriel, E & Young, S & Jayewardene, I & McPherson, B & Dooley, B 2013, 'Case study: assessment of the entrance stability of the Lake Illawarra estuary', In *14th Australasian Port and Harbour Conference*, Sydney.

Deltares 2014, '*Delft3D-Flow. Simulation of multi-dimensional hydrodynamic flows and transport phenomena, including sediments*', accessed 4 October 2016 <https://oss.deltares.nl/documents/183920/185723/Delft3D-FLOW_User_Manual.pdf>.

Fisher, K & Dawson, H 2013, '*Reducing Uncertainty in River Flood Conveyance. Roughness Review*', DEFRA / Environment Agency Flood and Coastal Defense R&D Program.

Haigh, I & Wadey, MP & Gallop, SL & Loehr, H & Nicholls, RJ & Horsburgh, K & Brown, JM & Bradshaw, E 2015, 'A user-friendly database of coastal flooding in the United Kingdom from 1915-2014', *Scientific Data*, vol. 2, article no 150021.

IPCC 2014, '*Climate Change 2014: Synthesis Report. Contribution of Working Groups I, II and III to the Fifth Assessment Report of the Intergovernmental Panel on Climate Change*', Core Writing Team: RK Pachauri & LA Meyer (eds.), IPCC, Geneva, Switzerland, 151pp.

Kaiser, G & Scheele, L & Kortenhaus, A & Loevholt, F & Römer, H & Leschka, S 2011, 'The influence of land cover roughness on the results of high resolution tsunami inundation modelling', *Natural Hazards and Earth System Sciences*, vol. 11, pp. 2521-2540.

Leonard, M & Westra, S & Phatak, A & Lambert, M & Van den Hurk, B & McInnes, K & Risbey, J & Schuster, S & Jakob, D & Stafford-Smith, M 2014, 'A compound event framework for understanding extreme impacts', *WIREs Climate Change*, vol. 5, pp. 113-128.

MHL 2012, '*NSW Tidal Planes Analysis 1990 - 2010 Harmonic Analysis*', Manly Hydraulics Laboratory, Report MHL2053, accessed 10 October 2016, <<http://new.mhl.nsw.gov.au/docs/oeh/tidalplanes/mhl2053%20OEH%20tidal%20plane%20analysis%20final%20report.pdf>>.

Miller, BM & Hawker, KM & Badenhop, AM 2006, '*Environmental flow modelling of salinity structure in the Shoalhaven estuary*', University of New South Wales, School of Civil and Environmental Engineering, Water Research Laboratory, Technical Report 2006/23, pp. 1-93.

Morris, B & Foulsham, E & Hanslow, D 2013, 'Quantifying tidal inundation variations in NSW estuaries', *In 22nd Coastal Conference*, Port Macquarie, accessed 10 April 2016 <<http://www.coastalconference.com/2013/papers2013/Brad%20Morris%20Full%20Paper.pdf>>.

Nielsen, P & Hanslow, DJ 1995, 'Wave setup at river entrances', *In 12th Australasian Coastal & Ocean Engineering Conference, combined with 5th Australasian Port & Harbour Conference*, accessed 10 June 2017, <<http://search.informit.com.au/documentSummary;dn=906525038211316;res=IELENG>>.

Olbert, A & Comer, J & Nash, S & Hartnett, M 2017, 'High-resolution multi-scale modelling of coastal flooding due to tides, storm surges and rivers inflows. A Cork City example', *Coastal Engineering*, vol. 121, pp. 278-296.

Poulter, B & Halpin, PN 2008, 'Raster modeling of coastal flooding from sea level rise', *International Journal of Geographic Information Sciences*, vol. 22, pp. 167-182.

Pugh, DT 2004, '*Changing sea levels: Effects of tides, weather and climate*', Cambridge, UK.

Ramirez, JA & Lichter, M & Coulthard, TJ & Skinner, C 2016, 'Hyper-resolution mapping of regional storm surge and tide flooding. Comparison of static and dynamic models', *Natural Hazards*, vol. 82, pp. 571-590.

Regena, C 2016, '*Quantifying the Physical and Biological Changes to Lake Illawarra, New South Wales, Due to Entrance Training*', Bachelor of Environmental Science (Honours), School of Earth & Environmental Sciences, University of Wollongong, accessed 3 May 2017, <<http://ro.uow.edu.au/thsci/138>>.

Resio, DT & Westerink, JJ 2008, 'Modeling the physics of storm surges', *Physics Today*, vol. 61, pp. 33-38.

Roy, PS & Williams, RJ & Jones, AR & Yassini, I & Gibbs, PJ & Coates, B & West, RJ & Scanes, PR & Hudson, JP & Nichol, S 2001, 'Structure and function of south-east Australian estuaries', *Estuarine Coastal and Shelf Science*, vol. 53, pp. 351-384.

Seenath, A & Wilson, M & Miller, K 2016, 'Hydrodynamic versus GIS modelling for coastal flood vulnerability assessment. Which is better for guiding coastal management?', *Ocean and Coastal Management*, vol. 120, pp. 99-109.

Short, AD & Woodroffe, CD 2009, '*The Coast of Australia*', Sydney, Australia.

Sloss, CR & Jones, BG & Murray-Wallace, C & Chenhall, BE 2004, 'Recent sedimentation and geomorphological changes, Lake Illawarra, NSW, Australia', *Wetlands (Australia)*, vol. 21, pp. 73-83.

Teng, J & Jakeman, AJ & Vaze, J & Croke, BFW & Dutta, D & Kim, S 2017, 'Flood inundation modelling: A review of methods, recent advances and uncertainty analysis', *Environmental Modelling and Software*, vol. 90, pp. 201-216.

Torres, JM & Bass, B & Irza, N & Fang, Z & Proft, J & Dawson, C & Kiani, M & Bedient, P 2015, 'Characterizing the hydraulic interactions of hurricane storm surge and rainfall-runoff for the Houston-Galveston region', *Coastal Engineering*, vol. 106, pp. 7-19.

Van de Sande, B & Lansen, J & Hoyng, C 2012, 'Sensitivity of coastal flood risk assessments to digital elevation models', *Water*, vol. 4, pp. 568-579.

Vitousek, S & Barnard, PL & Fletcher, CH & Frazer, N & Erikson, L & Storlazzi, CD 2017, 'Doubling of coastal flooding frequency within decades due to sea-level rise', *Scientific Reports*, vol. 7, pp. 1-9.

Vousdouskas, MI & Voukouvalas, E & Mentaschi, L & Dottori, F & Giardino, A & Bouziotas, D & Bianchi, A & Salamon, P & Feyen, L 2016, 'Developments in large-scale coastal flood hazard mapping', *Natural Hazards and Earth System Sciences*, vol. 16, pp. 1841–1853.

Wiecek, D & Regena, C & Laine, R & Williams, RJ 2016, 'Quantifying change and impacts to Lake Illawarra from a permanent opening, In *25th NSW Coastal Conference*, Coffs Harbour, accessed 20 February 2017 <<http://www.coastalconference.com/2016/papers2016/Lake%20Illawarra%20NSW%20Coastal%20Conference%20Paper-Wiecek%202016.pdf>>.

Woodroffe, CD & Buman, M & Kawase, K & Umitsu, M 2000, 'Estuarine infill and formation of deltaic plains, Shoalhaven River', *Wetlands*, vol. 18, pp. 72-84.

Zheng, F & Westra, S & Sisson, SA 2013, 'Quantifying the dependence between extreme rainfall and storm surge in coastal zones', *Journal of Hydrology*, vol. 505, pp. 172-187.